Energy Proceedings
2022
ISSN 2004-2965

Investigation of a Novel Cathode Flow Field of Proton Exchange Membrane Fuel Cell

Zhuo Zhang[1], Fan Bai[1], Pu He[1], Wen-Quan Tao[1*]

1 Key Laboratory of Thermo-Fluid Science & Engineering of MOE

Xi'an Jiaotong University, Xi'an, Shaanxi 710049, P R China

ABSTRACT

A good flow field design is important to the proton exchange membrane fuel cell (PEMFC) performance, especially under a high current density region, which is dominated by concentration polarization. Motivated by variable cross-section channel idea, in this study, a novel flow field containing a converging-diverging (C-D) pattern is proposed. A three-dimensional multiphase model with the novel flow field is established. The results show that it outperforms the conventional straight channel and depth-variant channel. The enhanced under land cross flow in novel flow field improve the reactant transport.

Keywords: flow field, converging-diverging, mass transport, performance improvement

1. INTRODUCTION

Under dual pressure of environmental protection and energy crisis, the PEMFC has become the research hotspot with the advantage features like high power density, high energy conversion efficiency, fast dynamic response, zero-emission and so on. Among the components, the flow field plate (FFP) or bipolar plate (BP), which plays an important role in the PEMFC stack, contribute the second biggest part of the whole PEMFC stack system cost [1]. Flow field design is a critical issue for BPs to be improved and optimized. As we all know, parallel, serpentine, interdigitated, and their combination flow field (here we call them 2D flow field) are widely used in commercial PEMFC bipolar plates. In 2014, Toyota released its first generation of fuel cell vehicles (FCV), MIRAI. In its fuel cell system, a 3D fine mesh flow field was developed. Unlike above mentioned 2D flow fields, the 3D flow field can promote gas transport to the cathode catalyst layer and quickly draw out the generated water [2]. Therefore, the 3D flow field attracted more and more attention. Cai et al. [3] and Shen et al. [4] presented a 3D flow field consisting of transport enhanced main channel, sub-channel, and transition areas. The simulation results showed the 3D flow field could enhance the mass transfer ability and improve the PEMFC performance. Besides, baffled flow channels are also an effective way to promote mass transfer [5].

3D flow field design has become a promising alternative for PEMFC, but a few issues remain with this approach. Zhang et al. [6] found that the 3D fine mesh flow field is not favorable to the PEMFC operating under the ohmic dominated region due to the decreased contact area between gas diffusion layer (GDL) may increase the ohmic loss. What's more, the existence of baffles made the manufacturing process of the flow field challenging and expensive because of the complex structure of baffles which leads to difficulties in the machining process.

Variable cross-section channels, which is between 2D and 3D flow field, could become the best promise to easy fabrication and mass transfer enhancement. Rezaie et al. [7] and Havaej [8] designed a flow field comprised of converging or diverging channels. Havaej [8] found that there was a gradient pressure from the converging channel towards its nearby diverging channel. The polarization curves show that by applying an angle of 0.3° to the channels, the net electrical output power increases by 16% compared to the straight base case [7].

We can see that the width and depth variation is beneficial for the PEMFC performance. Learning from this idea, we introduce the convergent-divergent structure at a local position in parallel channels and propose a novel flow field. Different from other variable cross-section channels, the width and depth of the channel change periodically and simultaneously along the flow direction. The objective is to improve mass transport and decrease concentration loss under high current density. The designed new flow field has the advantages of simple structure, easy processing, high output performance, fast drainage speed.

In this study, the three-dimensional (3D) multiphase model is adopted to simulate the cell performance with different flow fields. Net output power density is calculated considering the pumping loss, and under-land

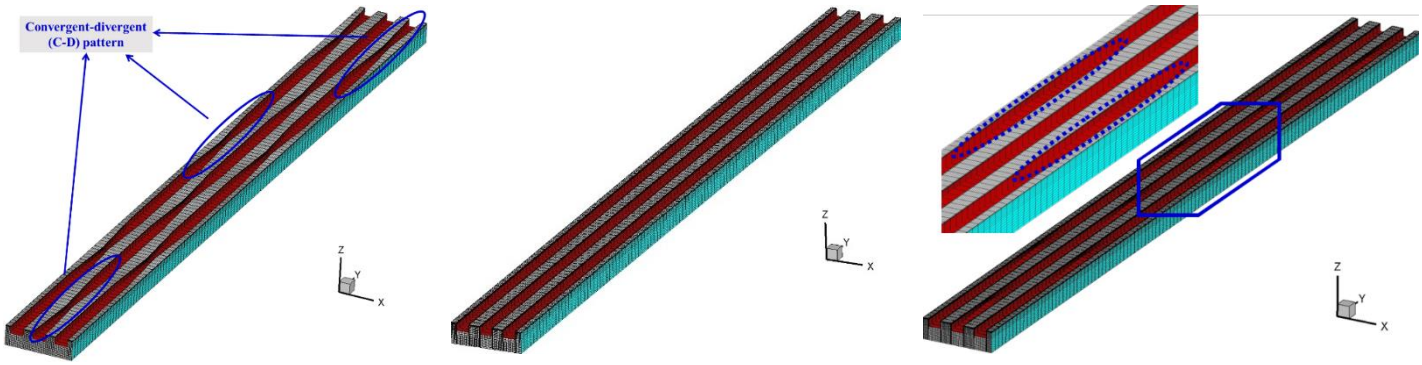

(a) Novel flow field plate *(b) Conventional flow field plate* *(c) Depth-variant flow field plate*

Fig. 1 Flow field plate

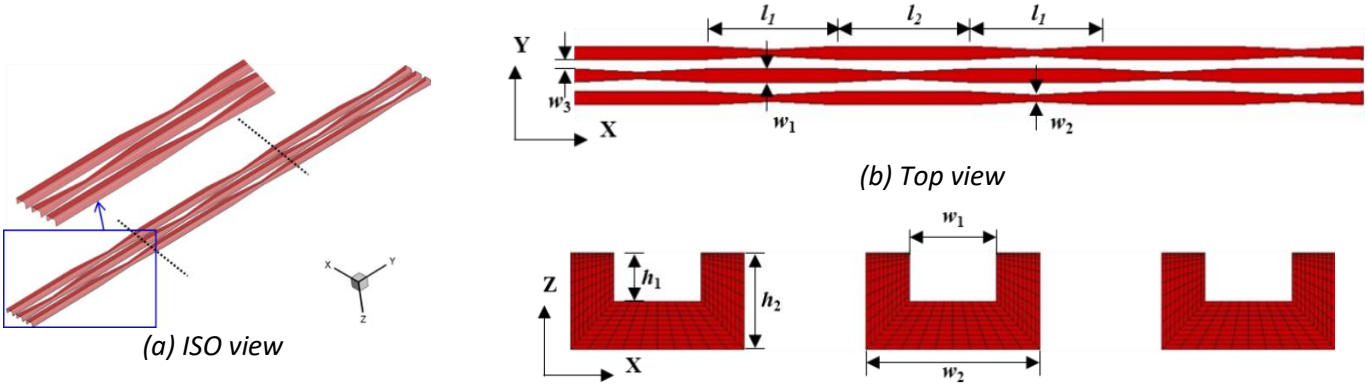

(a) ISO view

(b) Top view

(c) Front view

Fig. 2 Novel flow field

cross flow is revealed. The rest of the paper is organized as follows. The characteristic of the proposed novel flow field structure and numerical model is introduced in Section 2. The detailed results and discussion are presented in Section 3. Lastly, the main conclusions are summarized in Section 4.

2. MODEL DESCRIPTION

2.1 Novel flow field designs

The novel flow field plate we proposed is shown in Fig. 1(a), and the conventional straight and depth-variant flow field plates are also shown in Fig. 1(b) and (c) for comparison. The convergent-divergent (C-D) pattern is introduced periodically in novel flow field plate, while the cross-sectional area along flow direction remains unchanged in straight flow field plate. As shown in Fig. 2(a), the novel flow field could be regarded as an array of repeated unit. The black dotted line in Fig. 2(a) splits the flow field according to the repeated unit. Each channel in a repeated unit consists of a straight part and C-D part. The C-D pattern is staggered arranged between two adjacent channels, which ensures both straight and C-D parts are misaligned between adjacent channels. The related dimension of the novel flow field is annotated in Fig. 2 (b) (top view) and Fig. 2 (c) (front view). It is worth emphasizing that the width (from w_1 to w_2) and depth (from h_1 to h_2) of the channel both change linearly at C-D locations.

2.2 Computational domain

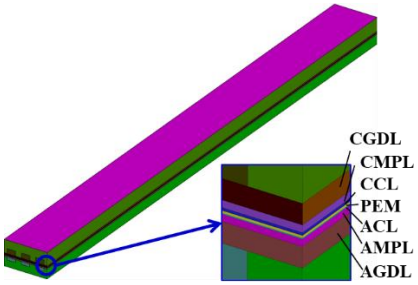

Fig. 3 Computational domain for 3D multiphase model

Fig.3 shows the computational domain in the performance simulation. It consists of BP, gas channel (GC, or flow field), GDL, microporous layer (MPL), catalyst layer (CL) in both anode and cathode sides. And a proton exchange membrane (PEM) zone is sandwiched in anode and cathode. Usually, the cell performance is limited by the cathode oxygen reduction reaction rate, especially under the concentration polarization region.

Therefore, the novel flow field we proposed is only adopted in the cathode, while the straight channel is always on the anode side. Both anode and cathode flow fields are made of 3 parallel channels.

2.3 Numerical models

The 3D two-fluid model is adopted to simulate the cell performance. Some assumptions are made, as follows,

(1) The fuel cell runs under a steady condition;

(2) The flow is laminar; Both the gas species and the gas mixture follow the ideal gas law;

(3) The amount of liquid water in channels is fixed as zero, assuming that the high gas velocity in the channel could blow out the liquid water completely.

(4) The contact resistance between different layers is ignored, which is employed in many modeling works.

Mass conservation equation (solved in GCs, GDLs, MPLs, CLs):

$$\nabla \cdot \left(\rho_{\mathrm{g}} \vec{u}_{\mathrm{g}} \right) = S_{\mathrm{m}} \tag{1}$$

Momentum conservation equation (solved in GCs, GDLs, MPLs, CLs):

$$\nabla \cdot \left(\frac{\rho_{\mathrm{g}} \vec{u}_{\mathrm{g}} \vec{u}_{\mathrm{g}}}{\varepsilon^2 \left(1-s_{\mathrm{lq}}\right)^2} \right) = -\nabla p_g + \mu_{\mathrm{g}} \nabla \cdot \left(\nabla \left(\frac{\vec{u}_{\mathrm{g}}}{\varepsilon \left(1-s_{\mathrm{lq}}\right)} \right) + \nabla \left(\frac{\vec{u}_{\mathrm{g}}^{\mathrm{T}}}{\varepsilon \left(1-s_{\mathrm{lq}}\right)} \right) \right) - \frac{2}{3} \mu_{\mathrm{g}} \nabla \left(\nabla \cdot \left(\frac{\vec{u}_{\mathrm{g}}}{\varepsilon \left(1-s_{\mathrm{lq}}\right)} \right) \right) + S_{\mathrm{u}} \tag{2}$$

Species conservation equation of *i*-species (solved in GCs, GDLs, MPLs, CLs): (*i*: H_2, O_2, water vapor)

$$\nabla \cdot \left(\rho_{\mathrm{g}} \vec{u}_{\mathrm{g}} Y_{\mathrm{i}} \right) = \nabla \cdot \left(\rho_{\mathrm{g}} D_{\mathrm{i}}^{\mathrm{eff}} \nabla Y_{\mathrm{i}} \right) + S_{\mathrm{i}} \tag{3}$$

Electrons conservation equation (solved in BPs, GDLs, MPLs, CLs):

$$0 = \nabla \cdot \left(\kappa_{\mathrm{ele}}^{\mathrm{eff}} \nabla \phi_{\mathrm{ele}} \right) + S_{\mathrm{ele}} \tag{4}$$

Protons conservation equation (solved in MEM, CLs):

$$0 = \nabla \cdot \left(\kappa_{\mathrm{ion}}^{\mathrm{eff}} \nabla \phi_{\mathrm{ion}} \right) + S_{\mathrm{ion}} \tag{5}$$

Liquid pressure conservation equation (solved in GDLs, MPLs, CLs):

$$0 = \nabla \cdot \left(\rho_{\mathrm{l}} \frac{K k_{\mathrm{lq}}}{\mu_{\mathrm{lq}}} \nabla p_{lq} \right) + S_{\mathrm{lq}} \tag{6}$$

Dissolved water conservation equation (solved in MEM, CLs):

$$\nabla \cdot \left(\frac{n_{\mathrm{d}}}{F} \nabla I_{\mathrm{ion}} \right) = \frac{\rho_{\mathrm{mem}}}{EW} \nabla \cdot \left(D_{\mathrm{mw}}^{\mathrm{eff}} \nabla \lambda_{\mathrm{mw}} \right) + S_{\mathrm{mw}} \tag{7}$$

Energy conservation equation (solved in the whole domain):

$$\nabla \cdot \left(\left(\rho C_{\mathrm{p}} \vec{u} \right)^{\mathrm{eff}} T \right) = \nabla \cdot \left(k^{\mathrm{eff}} \nabla T \right) + S_{\mathrm{E}} \tag{8}$$

where ρ_g, $\vec{u}_g$, Y_i, ϕ_{ele}, ϕ_{ion}, p_{lq}, λ_{mw}, T denote the gas density, gas mixture velocity vector, mass fraction of species *i*, electronic potential, proton potential, liquid pressure, membrane water content, and temperature, respectively.

stated above are solved by the finite volume method in the software ANSYS FLUENT. The user-defined functions (UDF) written by C code are implemented to update and customize source terms, transport properties, and boundary conditions during the solving process [9]. The expressions of the essential model parameters are given in Table 1.

Table 1 Model parameters and boundary conditions

Parameters	Value
Density of MEM(kg/m^3)	1980
Equivalent weight of MEM(kg/kmol)	1100
Porosities of GDL; MPL; CL	0.6;0.4;0.3
Contact angles of GDL; MPL; CL	110; 120; 95°
Intrinsic permeabilities of GDL; MPL; CL(m^2)	2.0×10^{-12}/1.0×10^{-12}/ 1.0×10^{-13}
Electrical conductivities of GDL; MPL; CL; BP(S/m)	6000/5000/ 5000/20000
Thermal conductivities of GDL; MPL; CL; MEM; BP(W/(m·K))	0.585;0.27; 0.27;0.109;129
Specific heat capacities of GDL; MPL; CL; MEM; BP(J/(kg·K))	861;800;240; 1287;710
Operating temperature(K)	353.15
Operating pressure (anode/cathode)(kPa)	50/50
Stoichiometric ratio (anode/cathode)	1.5/1.5
Relative humidity	100%/100%
Reference exchange current density(A/m^3)	3.0×10^7/30.0
Reference H_2/O_2 concentration(kmol/m^3)	56.4/40.0
Transfer coefficient	0.5/1.0

3. RESULTS AND DISCUSSION

3.1 Performance improvement

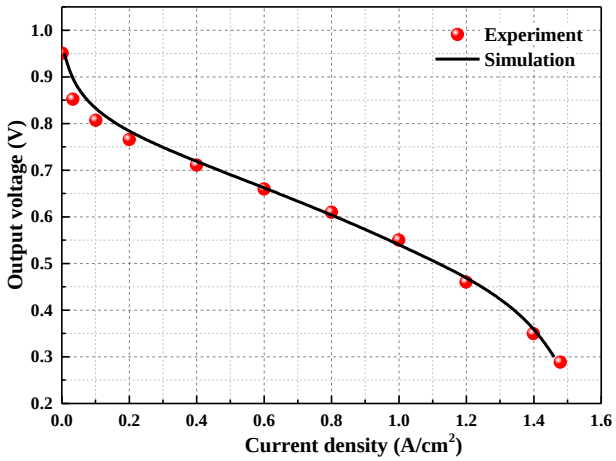

Fig. 4 Model validation

The simulated polarization curve is compared with the test data in Ref.[10] under the same operating condition. As shown in Fig. 4, the predicted polarization curve is in good agreement with the experiment data, which validated our model accuracy.

Based on the validated 3D multiphase model, we simulated the cell performance with different cathode flow fields, as shown in Fig. 5. Compared with the depth-variant flow field, the novel flow field can further improve the performance, especially in the concentration polarization region. This indicates channel with both width and depth variation outperforms the channel with only depth variation (e.g. 3D wave channel [11]). Under the same output current density 2.0 A/cm^2, the output voltage or the total power density of novel and depth-variant flow field increase about 25.2% and 14.2%, respectively.

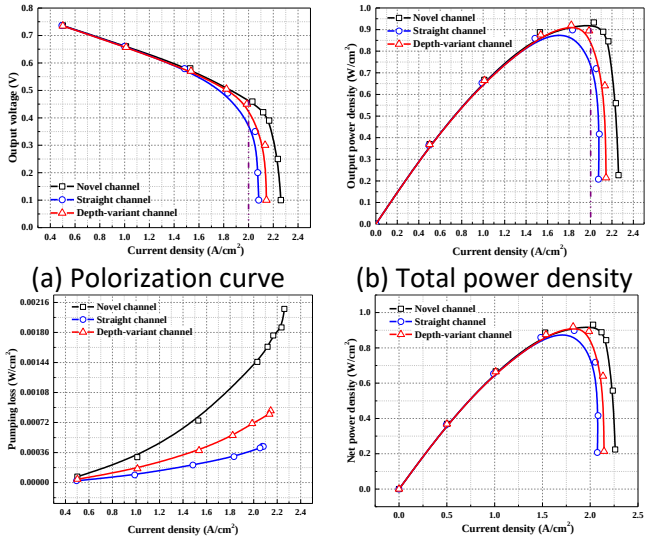

(a) Polorization curve (b) Total power density

(c) Pumping loss (d)Net output power density

Fig. 5 Performance comparison of the different flow field

After the C-D pattern is applied in the cathode flow field, the pump power in the cathode channel would increase, as shown in Fig. 5(c). The pumping loss W_{pump} is calculated by

$$W_{\text{pump}} = \frac{\Delta p q_v}{A_{\text{act}} \zeta} \tag{9}$$

Although the pumping loss of the novel cathode flow field is higher than the conventional straight one, it is rather small (two orders of magnitudes lower) compared with the total output power density. As a result, the novel flow field still takes advantage in net output power density, as shown in Fig. 5(d).

3.2 Under land cross flow

Under land cross flow in PEMFC, which is in favor of reactant transport, has been observed by many researchers. The staggered arrangement of C-D in a novel flow field also induces the cross flow.

Fig. 6(a) and 6(b) represents the contour of gas velocity in the cathode flow field. The local high speed (about 7 m/s) can be observed near the C-D location in the novel flow field (Fig. 6(b)), while in the straight flow field, it maintains a relatively uniform low velocity (about 2 m/s) field (Fig. 6(a)). Furthermore, different flow characteristics cause different pressure distributions, as shown in Fig. 6(c) and 6(d). The pressure decreases monotonously from channel inlet to channel outlet in the straight flow field. The novel flow field presents a scale-like pressure distribution by contrast. That means there always exists a pressure difference between two adjacent flow channels along the flow direction.

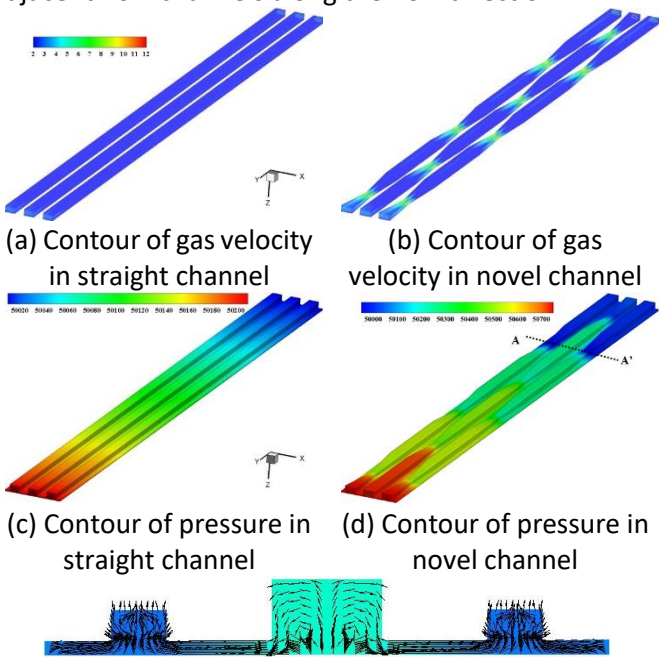

(a) Contour of gas velocity in straight channel

(b) Contour of gas velocity in novel channel

(c) Contour of pressure in straight channel

(d) Contour of pressure in novel channel

(e) Contour of A-A' pressure and velocity vector (only direction) in novel channel

Fig. 6 Gas velocity in the straight and different flow field

As shown in Fig. 6(e), we extracted the A-A' cross-section and plotted the velocity vector on that. The pressure difference induces the under land cross flow through the gas diffusion layer obviously. This convection flux is a benefit for reactant gas transport and liquid water drainage. In a straight channel, only the diffusion caused by concentration difference can cause the gas transport from the channel to the catalyst layer.

CONCLUSIONS

In this work, a novel flow field that can promote mass transfer and improve cell performance is proposed. The 3D multiphase model is adopted to simulate the output performance. The main findings of this study are as follows.

(1) The total power density of the novel flow field can improve performance by about 25.2% under the same output current density 2.0 A/cm^2. After subtracting the pumping loss, the net power density is still greatly improved.

(2) The novel flow field could enhance the under land cross flow. This is beneficial to the reactant transport under concentration difference dominant zone.

ACKNOWLEDGEMENT

Following funds are greatly acknowledged: The grant from the Key Project of National Natural Science Foundation of China (51836005, 51911530157), the Basic Research Project of Shaanxi Province (2019ZDXM3-01), and the 111 project (B16038).

REFERENCE

[1] Wang Y, Ruiz Diaz DF, Chen KS, Wang Z, Adroher XC. Materials, technological status, and fundamentals of PEM fuel cells – A review. Materials Today. 2020;32:178-203.

[2] [1] Yoshida T, Kojima K. Toyota MIRAI Fuel Cell Vehicle and Progress Toward a Future Hydrogen Society. Interface magazine. 2015;24(2):45-9.

[3] Cai Y, Fang Z, Chen B, Yang T, Tu Z. Numerical study on a novel 3D cathode flow field and evaluation criteria for the PEM fuel cell design. Energy. 2018;161:28-37.

[4] Shen J, Tu Z, Chan SH. Performance enhancement in a proton exchange membrane fuel cell with a novel 3D flow field. Applied Thermal Engineering. 2020;164:114464.

[5] Cai Y, Wu D, Sun J, Chen B. The effect of cathode channel blockages on the enhanced mass transfer and performance of PEMFC. Energy. 2021;222:119951.

[6] Zhang G, Xie B, Bao Z, Niu Z, Jiao K. Multi-phase simulation of proton exchange membrane fuel cell with 3D fine mesh flow field. International Journal of Energy Research. 2018;42(15):4697-709.

[7] Zehtabiyan-Rezaie N, Arefian A, Kermani MJ, Noughabi AK, Abdollahzadeh M. Effect of flow field with converging and diverging channels on proton exchange membrane fuel cell performance. Energy Conversion and Management. 2017;152:31-44.

[8] Havaej P. A numerical investigation of the performance of Polymer Electrolyte Membrane fuel cell with the converging-diverging flow field using two-phase flow modeling. Energy. 2019;182:656-72.

[9] He P, Mu Y-T, Park JW, Tao W-Q. Modeling of the effects of cathode catalyst layer design parameters on performance of polymer electrolyte membrane fuel cell. Applied Energy. 2020;277:115555.

[10] Ozen DN, Timurkutluk B, Altinisik K. Effects of operation temperature and reactant gas humidity levels on performance of PEM fuel cells. Renewable and Sustainable Energy Reviews. 2016;59:1298-306.

[11] Chen X, Yu Z, Yang C, Chen Y, Jin C, Ding Y, et al. Performance investigation on a novel 3D wave flow channel design for PEMFC. International Journal of Hydrogen Energy. 2021;46(19):11127-39.